Ground motion prediction equations

Report

Author(s):
Edwards, Benjamin; Fäh, Donat

Publication date:
2014-09-11

Permanent link:
https://doi.org/10.3929/ethz-a-010232326

Originally published in:
SED report SED/ENSI/R/01/20140911

Schweizerischer Erdbebendienst
Service Sismologique Suisse
Servizio Sismico Svizzero
Servizi da Terratrembels Svizzer

ETH
Eidgenössische Technische Hochschule Zürich
Swiss Federal Institute of Technology Zurich

Ground Motion Prediction Equations

SED Report SED/ENSI/R/01/20140911

Benjamin Edwards and Donat Fäh

Swiss Seismological Service, ETH Zürich

11/9/2014

DOI: 10.3929/ethz-a-010232326

Table of Contents

Summary

This report provides a brief overview of the state-of-the-art in ground motion prediction as currently used in probabilistic seismic hazard analysis (PSHA) projects. A focus is on models used for predictions in Switzerland and the issues surrounding their use and adjustment. Empirical approaches and simulation approaches are discussed in addition to problems related to their implementation in local or regional projects. Finally the outlook and trends in this field are summarised.

1 Introduction

A ground motion prediction equation (GMPE) is a generic term for an equation providing a statistical estimate of the expected ground motion and its standard deviation due to a given earthquake scenario. The measure of ground-motion provided by a GMPE is typically the 5% damped relative pseudo-spectral acceleration (PSA). 5% damped PSA is given by the product of the squared angular frequency (ω^2) and the absolute spectral displacement (SD) of a simple harmonic oscillator, damped to 5% of critical. GMPEs sometimes also provide other measures of ground-motion such as SD, relative pseudo-spectral velocity (PSV = ωSD), peak ground acceleration (PGA) or peak ground velocity (PGV). The purpose of these choices is to represent the response of simple structures (e.g., residential buildings) to ground-shaking and therefore provide useful input for engineering applications. Different choices of damping and period have a significant impact on the response.

Since observed ground motion for a given scenario is log-normally distributed, GMPEs provide output (ground-motion measure and standard deviation) either as natural or base-10 logarithm. Whilst the truncation of ground-motion distributions (i.e., maximum possible ground-motion; not to be confused with soil non-linearity or maximum earthquake magnitude) is considered intuitive, for instance due to limiting material properties, it is typically not considered in seismic hazard. It is important to note that the units of ground motion provided by GMPEs are not standardized (e.g., SI units). Authors present GMPEs in terms of SI units (m, m/s, m/s2), CGS units (cm, cm/s, cm/s2 or gal) or, for PSA, sometimes in terms of units of gravity. The combination of possible output, unit convention and logarithm types (which are not necessarily always clear in publications) means that users of GMPEs should be careful to understand exactly how a GMPE should be implemented.

GMPEs are determined based on either empirical or simulated data. In both cases a simplified functional form (the GMPE) is fit to a dataset. The form of GMPEs is typically:

$$\log(Y) = f_{source}(M) + f_{path}(R, M) + f_{site}(Vs30, \ldots) + \varepsilon\sigma \quad (1)$$

Here Y is the measure of ground-motion (PSA, PSV, SD at given period (T), or PGA, PGV, etc.). f_{source} is a function that appropriately scales ground-motion with magnitude, f_{path} is a function accounting for attenuation, and f_{site} is a function that accounts for local effects (e.g., amplification) at the recording site. M is the magnitude (typically moment magnitude) and R is a source-site distance measure. f_{site} is typically parameterised using basic site descriptors, such as the average shear-wave velocity of the upper 30m ($Vs30$), Eurocode 8 site class (CEN, 2004) and sediment thickness. Finally $\varepsilon\sigma$ describes the variability of the ground-motion: a log-normal distribution with zero mean and standard-deviation equal to σ. Examples of recent GMPEs are shown in Figure 1.

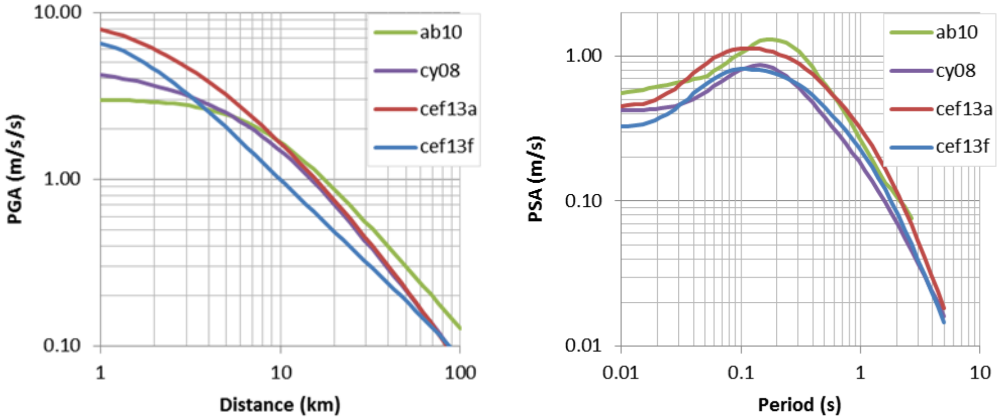

Figure 1: Example of GMPEs. Left: PGA versus distance for a magnitude 6 strike-slip earthquake recorded at a hard-rock site (Vs30=1100m/s). Right: PSA versus period for a magnitude 6 strike-slip earthquake recorded at 30km distance at a hard-rock site (Vs30=1100m/s). Key: ab10 (Akkar and Bommer, 2010); cy08 (Chiou and Youngs, 2008); cef13a (Cauzzi *et al.*, submitted, 2014) Swiss alpine model; cef13f (Cauzzi *et al.*, submitted, 2014) Swiss foreland model.

An important consideration is that the functional form of a GMPE can quickly become over-parameterised, or include unrealistic elements, which create problems at the edge of data-coverage. An analogy is fitting a high-degree polynomial to a scatter plot: the polynomial may fit the data very well, but is not robust at the extremes of the dataset and leads to erratic extrapolation beyond (Zhao and Lu, 2011). For this reason empirical models should only be used with input parameters that lie within the range of values used in their derivation: if a GMPE was developed using events with $4.5 < \boldsymbol{M} < 7$ then it should only be used to predict ground motions within this range (preferably with some degree of conservatism to avoid the less robust model space). The same consideration should be applied for all other input terms (distance, Vs30, etc.).

Overly complex models may provide no benefit if the input metadata available is limited: in this case conversions, estimates or default values must be used in order to provide all input parameters required for the GMPE. Consequently the related uncertainty should be propagated to the final ground-motion estimate. An example of this would be if only the expected hypocentral distance was known for a scenario event: for a GMPE based on rupture distance we must make predictions for the range of possible rupture distances consistent with the known hypocentral distance. The resulting suite of GMPE estimates using all possible equivalent rupture distances represents the probability distribution of ground-motion estimates for the given scenario. It is therefore clear that a balance between functional form complexity and user requirements is necessary: the best GMPE for a given application may not be the most complex.

A set of recommendations regarding selection of GMPEs (e.g., on functional form) are made by Bommer et al. (2010) and Cotton et al. (2006), which are typically followed in Senior Seismic Hazard Analysis Committee (SSHAC, 1997) Level 3 or 4 projects [e.g., in the Pegasos Refinement Project (PRP) or Seismic Harmonization in Europe (SHARE) project]. Effective criteria were presented by Bommer et al. (2010), who proposed to exclude GMPEs from PSHA if:

1. The model is derived for an inappropriate tectonic environment.
2. The model is not published in a Thomson Reuters ISI-listed peer reviewed journal (although an exception can be made for an update to a model that did meet this criterion).

3. The dataset used to derive the model is not presented in a table listing the earthquakes and their characteristics, together with the number of records from each event.
4. The model has been superseded by a more recent publication.
5. The model does not provide spectral predictions for an adequate range of response periods.
6. The functional form lacks either non-linear magnitude dependence or magnitude-dependent decay with distance.
7. The coefficients of the model were not determined with a method that accounts for inter-event and intra-event components of variability; in other words, models must be derived using one- or two-stage maximum likelihood approaches or the random effects approach.
8. Model uses inappropriate definitions for explanatory variables, such as M_L or R_{epi}, or models site effects without consideration of site characterization, such as Vs30.
9. The range of applicability of the model is too small to be useful for the extrapolations generally required in PSHA: $M_{min} > 5$, $M_{max} < 7$, $R_{max} < 80$ km.
10. Model constrained with insufficiently large dataset: fewer than 10 earthquakes per unit of magnitude or fewer than 100 records per 100 km of distance.

An overview of the functional forms and important features of GMPEs developed between 1964 and 2010 is presented by Douglas (2011) and Douglas (2014) with accompanying online resource www.gmpe.org.uk (last accessed Sept. 2014).

2 Empirical GMPEs

Empirical models are defined here as models based on a majority of empirical data. They use simplified functional forms to model recorded data in a robust manner. Their functional forms are based on broad simplifications of our physical understanding of the scaling properties of input variables (e.g., magnitude, distance, Vs30).

2.1 Source

The source term of GMPEs is the most ubiquitous – in the majority of cases it is given by:

$$f_{source}(\boldsymbol{M}) = c_1 + c_2\boldsymbol{M} + c_3\boldsymbol{M}^2 + f_{Mech} \quad (2)$$

Where c_{1-3} are regression coefficients. Non-linear (typically quadratic) magnitude scaling of ground-motion is not always apparent in strong-motion datasets (e.g., Zhao *et al.*, 2006, Cauzzi and Faccioli, 2008) possibly due to trade-off or large aleatory variability. However, GMPEs with linear magnitude scaling are typically discounted as unrealistic (Bommer *et al.*, 2010). Non-linear magnitude scaling and the functional form in Equation (2) was introduced by Fukushima (1996). They found that non-linear scaling was required in order to adequately reflect the period- and source corner-frequency dependent scaling of Fourier spectral amplitudes with Moment Magnitude. They used simple Brune (1970) ω^2 earthquake source models to show that linear scaling ($c_1 + c_2\boldsymbol{M}$) was insufficient due to the reduction of source corner-frequencies with increasing magnitude. Although Fukushima's study was based on Fourier amplitudes, at periods of typical engineering interest (e.g., 0.1s to 5s) they closely reflect the behaviour of damped response spectral amplitudes (used in GMPEs). A physical basis therefore exists to justify non-linear magnitude scaling of response spectral ordinates, which can be approximated as a quadratic. This can be seen in Figure 2, where ω^2 source based simulations [smsim; (Boore, 2003)] from Edwards and Fäh (2013b) are included alongside parametric GMPEs using quadratic magnitude scaling. At shorter periods the correspondence between the Fourier spectrum and response spectrum becomes non-linear, depending to an increasing extent on the damped oscillator response. Nevertheless, the same quadratic form for $f_{source}(\boldsymbol{M})$ is typically used by most authors throughout the period range.

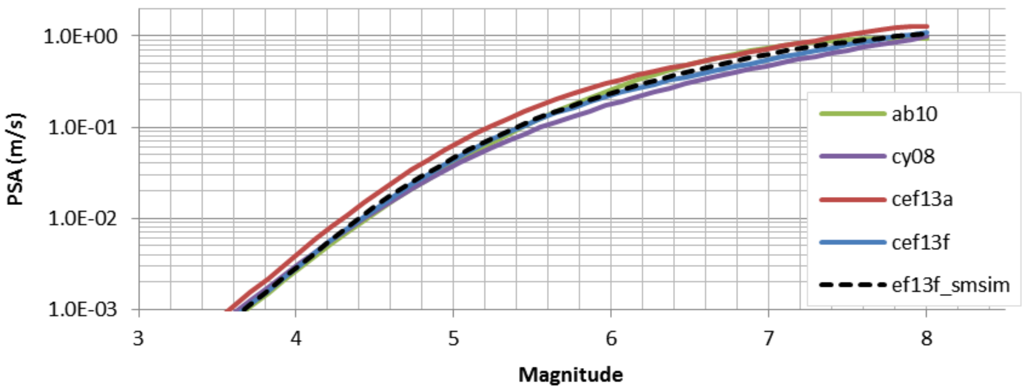

Figure 2: Example of source magnitude scaling in GMPEs for T=1s and R=30km for a strike-slip earthquake recorded at a hard-rock site (Vs30=1100m/s). Key: ab10 (Akkar and Bommer, 2010); cy08 (Chiou and Youngs); cef13a (Cauzzi *et al.*, submitted, 2014) Swiss alpine model; cef13f (Cauzzi *et al.*, submitted, 2014) Swiss foreland model; ef13f_smsim (Edwards and Fäh, 2013b) Swiss foreland simulations.

In addition to the non-linear magnitude scaling, nearly all GMPEs include a style of faulting term (f_{Mech}: which varies depending on normal, strike-slip or reverse/thrust source mechanisms). Studies typically find that ground motions from normal faults are lowest, while reverse or thrust faults lead to higher ground-motion for a given distance. Some GMPEs also include hanging or footwall terms (Figure 3) which account for the inability of particular distance metrics (e.g., rupture distance) to account for the increased ground-motion on the hanging-wall of reverse earthquakes due to the close proximity of a large area of the ruptured fault (Abrahamson and Somerville, 1996). The Joyner-Boore distance (distance to the surface projection of the fault plane: see section 4 Distance Measures) can account somewhat for the hanging wall effect since all points above the fault plane have zero distance.

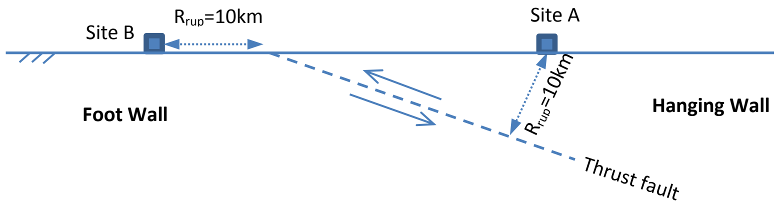

Figure 3: Hanging wall effect. Cross section of a scenario for shallow dip reverse (thrust) faults: site A and B have the same distance to the rupture R_{rup}=10km. However, site A experiences stronger ground-shaking due to the closer proximity of the extended fault plane. Other distance metrics, such as the Joyner-Boore distance (see section 4 Distance Measures) can account for this better: e.g.: for site A (stronger shaking) R_{JB}=0km and site B R_{JB} = 10km.

2.2 Path

The attenuation term in GMPEs varies from author to author. However, a common feature is that there are components modelling geometric and, in some cases anelastic, decay. Geometric decay is modelled with a magnitude dependence to capture the reduction of geometrical decay for increasingly large fault sizes (Cotton *et al.*, 2008).

An example of the path component is:

$$f_{path}(R, \boldsymbol{M}) = (c_4 + c_5\boldsymbol{M})\log(R) + c_6 R \quad (3)$$

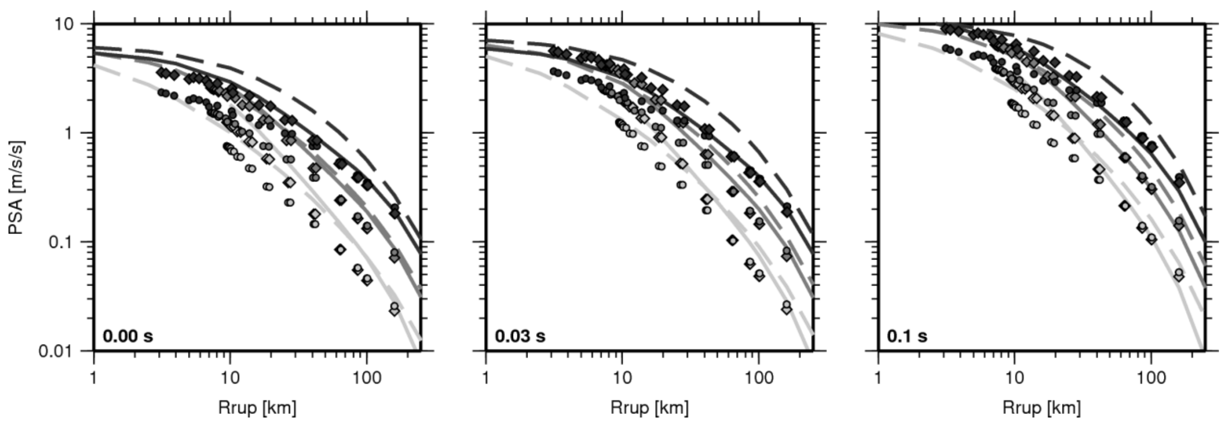

Figure 4: Example of magnitude dependent path attenuation caused by increasing fault size. Shown at different periods, for events with M_w 5.5 (light grey), 6.5 (gray), and 7.5 (dark grey). Simulations are shown for the Swiss Foreland (circles) and Alpine (diamonds) (Edwards and Fäh, 2013b) and the GMPEs of Chiou and Youngs (2008, solid lines) and Zhao et al., (2006, dashed lines). Note the apparent decrease of attenuation for the larger magnitude events.

where regression coefficients c_{4-5} control the magnitude dependent geometrical decay and c_6 controls the anelastic decay (which may or may not be included). The anelastic decay term is closely associated to the quality factor (Q), however physical interpretation in this respect is limited due to the broad sensitivity of high frequency PSA (i.e., high oscillator frequencies) to lower frequency ground motions. As we approach a large fault the dominant contribution to ground motion comes from a limited extent of the fault rupture (i.e., high frequency ground-motions from the distant parts of the fault are strongly diminished with respect to those originating nearby). For the distance term a near-fault saturation effect (e.g., $R = \sqrt{R_{rup} + c_7}$) is therefore often implemented.

2.3 Site

Site terms in GMPEs are the most variable between different authors, from the most simple which use only site class (e.g., hard-rock, rock, stiff-soil, soil, soft-soil), to those which include a number of continuous geotechnical site classification parameters such as an average shear-wave velocity (e.g., the upper 30m travel-time average velocity: Vs30) or depth to the underlying bedrock. For this reason the details of site-specific effects in GMPEs are not discussed in detail here. Nevertheless, all GMPEs effectively provide a smoothed average site-amplification term that is consistent with the input classification terms and background dataset. It is typically assumed that this implicitly defines a site reference (the host reference site) (Campbell, 2003). Consequently adjustments from one site type to another (generally a well-studied local site) are possible (see section 7 GMPE Adjustment). An issue related to this so called host-to-target adjustment is that the sites used in the development of GMPEs are often not characterized in detail. For instance, simple (and often unreliable) proxies such as site topography (e.g., slope) or geology may have been used to assign Vs30 values. This may result in systematic differences in site classification from region to region, depending on practices and methodologies.

A limitation of simple classification approaches (e.g., site type or Vs30 values) is that they do not fully reflect the amplification behaviour of a site. For instance, a typical stiff-soil (360<Vs30<800m/s) site in California may respond to input ground-motion differently to a similarly classified site in Switzerland. The reason for this can be related to geology: a region dominated by deep sedimentary basins, for example, will introduce stronger long-period amplification for a given site class. The Swiss seismological service currently makes detailed site classification including the determination of full velocity profiles and related amplification for all new strong-motion sites installed in Switzerland using a variety of approaches (Michel *et al.*, 2014). This process reduces epistemic uncertainty in GMPEs.

For site-specific analyses (deterministic or probabilistic) the amplification within a GMPE (e.g., based on input Vs30 or site class, Figure 5) is rarely appropriate and will likely introduce bias when compared to local data. Host-to-site adjustment, which removes the smooth average GMPE reference amplification and replaces it with a locally derived model, is therefore critical (as discussed in more detail later).

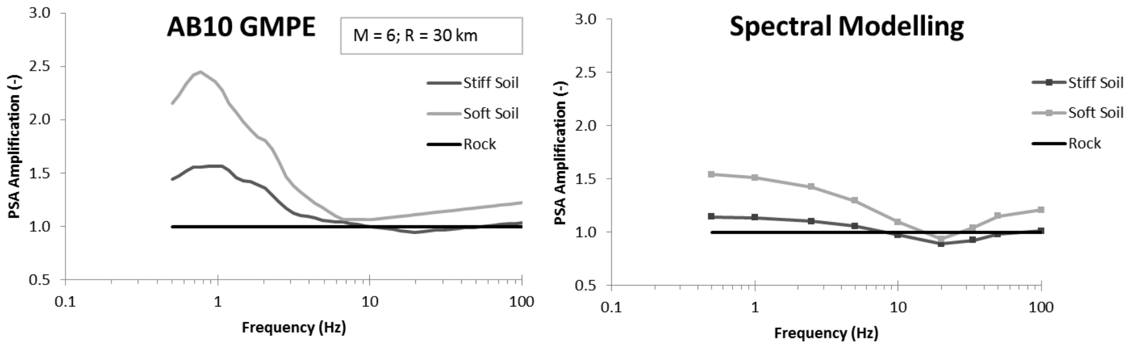

Figure 5: Average amplification at soft- and stiff-soil sites with respect to rock in the GMPE of Akkar and Bommer (2010). Left: directly from the GMPE; right: from spectral modelling (Edwards and Fäh, 2013a). Note that the standard deviations are not indicated due to being very large: site to site variability is significant.

2.4 Vertical Ground Motions and the V/H Ratio

The vertical component of ground motion can have a significant effect on the seismic response of particular structures, such as bridges. Beyond a few examples, GMPEs are not typically available for the vertical component of ground-motion. Nevertheless, it may actually be beneficial to use a GMPE for the horizontal component of motion in combination with a vertical to horizontal (V/H) ratio. In this case, PSHA or scenario modelling is undertaken solely using the horizontal component of ground motion, and the resulting design spectra are later adjusted to the vertical orientation. The resulting horizontal and vertical design spectra will then both correspond to the same earthquake (disaggregation) scenario (Gulerce and Abrahamson, 2011). V/H ratio models are typically developed in the same fashion as GMPEs, with a simple linear sum of components representing source, path and site and using V/H ratio data. Examples (as used in the Pegasos Refinement Project) include Bommer et al. (2011) and Campbell and Bozorgnia (2003).

Since the V/H ratio is primarily driven by site effects (with minor contributions due to the proportion of P- and S-waves), Edwards et al. (2011b) developed a predictive V/H model for rock sites using whole the shear-wave velocity profile as input (through the quarter-wavelength approach). This built on previous empirical approaches based only on Vs30. Subsequently, Poggi et al. (2012a) extended the model to soil and sedimentary sites by introducing the quarter-wavelength impedance contrast parameter as a predictor variable. This approach allows the full Vs profile to be included along with information about resonance (which strongly affects the V/H ratio for low velocity sites).

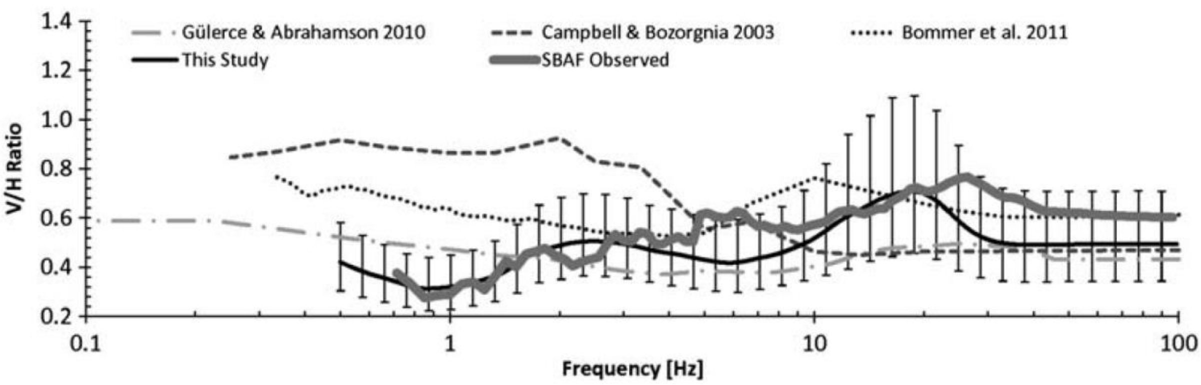

Figure 6: Comparison of V/H models and a Swiss strong-motion installation site (SBAF). Reproduced from Poggi et al. (2012a).

3 Simulation Models

Simulation based models currently used for ground motion prediction in seismic hazard analysis are based on stochastic representation of an earthquake acceleration time series (Boore, 2009, Boore, 2003). The stochastic accelerogram is comprised of a random phase Gaussian signal, convolved with Fourier spectrum based models of the earthquake source, attenuation and site effects. In practice, if only the response spectrum is required (not the whole time-series), random vibration theory is used to extract the peak values for given oscillator periods (Cartwright and Longuet-Higgins, 1956). More complex simulation models are used for deterministic earthquake scenarios, but are generally not yet used in seismic hazard analyses due to high uncertainties related to input parameters and their associated covariance. Such models, and hybrid models (e.g., Mai *et al.*, 2010) which combine deterministic and stochastic simulation approaches, will play an important role in future hazard projects as uncertainties are decreased. However, they are not further discussed in this report which focusses on current practice.

Some authors have developed parametric GMPEs (as for empirical models) based on stochastic simulations with random sampling of input parameters from their statistical distributions (e.g., Atkinson and Boore, 2006). The uncertainty estimates from such models are generally debated due to strong simulation parameter covariance (Rietbrock *et al.*, 2013). Other simulation models develop median predictions and estimate uncertainty through residual analyses using local data or the adoption of global uncertainty models (e.g., Edwards and Fäh, 2013b).

3.1 Source

As for the quadratic magnitude scaling in empirical GMPEs, source models for stochastic simulation are usually based on a simple model proposed by Brune (1970, 1971). This model describes the far-field representation of an instantaneously-slipping fault using a limited number of parameters: seismic moment and corner-frequency (earthquake dependent), radiation coefficient (azimuth dependent) and a number of terms usually assumed constant (e.g., density, velocity, etc.). Other models are available, with either adjustments for locally observed events (e.g., Atkinson, 1993) or more general models with added complexity, such as two-corner models (Atkinson, 1993), or non-instantaneous slip models (accounting for fault finiteness and stopping phases) (Madariaga, 1976). Such models, however, may introduce complexity that cannot be justified in the case of non-deterministic applications.

To account for the finite extent of faults for large magnitude events two approaches are used: direct simulation using a distribution of point-sources (Motazedian and Atkinson, 2005, Atkinson and Boore, 2006) or geometrical effects, similar to those used in empirical GMPEs (Edwards and Fäh, 2013b, Rietbrock *et al.*, 2013). Distributed point source models are the most complex and can include effects such as directivity, however, they include a significant number of additional parameters (primarily hypocentre location and slip distribution). On the other hand, geometrical adjustments such as the effective distance [R_{eff}, (Boore, 2009)] have been shown to result in negligible differences to the finite fault models in the case that the hypocentre and slip are randomised (as is typical in probabilistic seismic hazard).

3.2 Path

Path effects are a function of the source-site propagation path: typically simplified as a function of a distance metric (R), and sometimes including source depth. Two main processes attenuate the amplitude of seismic waves along the propagation path: intrinsic and scattering attenuation [described by Q (Knopoff, 1964): amplitude ∝ exp(-πfR/(βQ)), with β the average propagation velocity] and geometrical attenuation (e.g., amplitude ∝ 1/R for a spherically expanding wave-front). The two effects prove difficult to resolve using locally recorded data due to strong trade-offs (Morozov, 2008). To overcome this, frequency dependent Q is often determined based on an assumed geometrical decay. Alternatively, other authors determine Q based on the spectral shape, and then determine geometrical decay in a subsequent stage (e.g., Figure 7). This approach can highlight effects due to crustal structure such as depth varying Q, and reflections from the bottom of the crust (Edwards *et al.*, 2011a). For instance, in Switzerland, the deeper Moho in the alpine region, coupled with the shallower seismicity, means that post-critical SmS reflection phases (strong reflections from the mantle) are observed at greater distances than in the foreland. The observance of SmS reflections appears to reduce the decay of seismic energy with respect to distance (Figure 7). Such detailed features of wave-propagation effects are a feature of simulation models based on regional seismicity: they are not included in empirical GMPEs as data is taken from a wide range of regions.

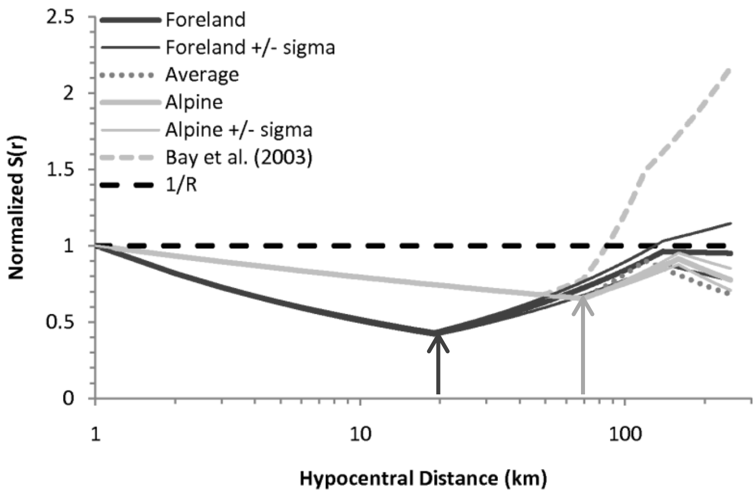

Figure 7: Example of apparent geometrical decay [S(r)] for the Swiss alpine and foreland regions (normalized by 1/R). The arrows mark the closest (average) observance of change in attenuation in both regions (e.g., due to SmS reflections).

When simulating ground-motions, it is important to take path effects that are consistent and not based on different assumptions: ideally geometric attenuation and Q should be sourced from a single study, or if epistemic uncertainty is explored, pairs of parameters (Q and geometrical effects) should be treated as strongly covariate.

3.3 Site

Simulation approaches are significantly more flexible than empirical GMPEs in that location or region specific features of wave-propagation can be incorporated into the predictive models. Source and path effects are generally rather uncertain (due to strong trade-offs and modelling assumptions used to derive them). Consequently simplified models are generally favoured. On the other hand, the determination of site amplification is more robust (with quantifiable uncertainty) since estimates can be obtained based on several independent geophysical investigations: direct inversion (e.g., Edwards *et al.*, 2013), noise analysis (e.g., Poggi *et al.*, 2012b), and seismic surveys (Fäh *et al.*, 2009).

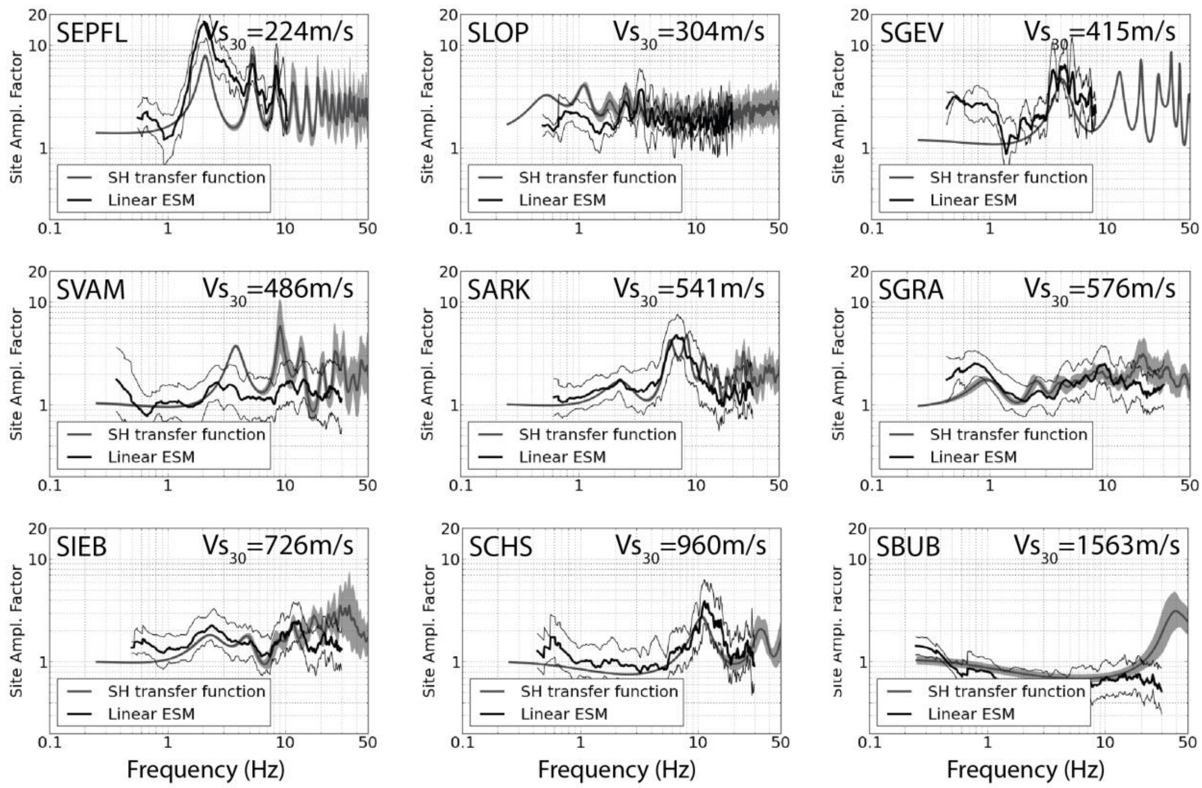

Figure 8: Comparison between theoretical 1D SH transfer function from site characterization velocity profiles and empirical elastic amplification (ESM) for selected Swiss sites exhibiting 1D amplification behavior (ordered by increasing Vs_{30})

Using amplification that is locally referenced should be avoided for ground-motion prediction at regional scales. Locally referenced amplification models include theoretical SH-amplification between the local bedrock and the surface or site-to-reference spectral ratios (i.e., a nearby hard-rock reference). With such approaches the additional variability of the local reference condition is mapped into the prediction uncertainty and introduces ambiguity or bias in setting a global reference for forward simulation or host-target adjustment. Instead, a common crustal reference velocity model should be defined for simulation approaches (Poggi *et al.*, 2011, Poggi *et al.*, 2013, Boore and Joyner, 1997). This reference then accounts for the amplification due to the velocity structure of the crust (e.g., 4km depth to bedrock). Site-specific amplification (due to soil and weathered rock layers, linear or non-linear) relative to the defined reference model is then applied depending on the local velocity and material property structure of the subsurface (e.g., Figure 8). In this way the resulting simulations are explicitly referenced to a known crustal velocity model, and reflect the significant variability of possible effects (e.g., resonance at particular frequencies, non-linearity, 2D and 3D effects) of the near-subsurface on ground-motion.

4 Distance Measures

The choice of distance measure to be used with a GMPE (either empirical or simulation based) lies with the developer. Several commonly used distance metrics are available and each has advantages and disadvantages. When using a GMPE the user must input the same distance metric that it was designed for. This may mean that conversions (e.g., Scherbaum *et al.*, 2004) have to be applied to a user's database or modelling approach before predictions can be made. In the case that conversions are used the propagation of uncertainty to the ground-motion estimate must also be considered.

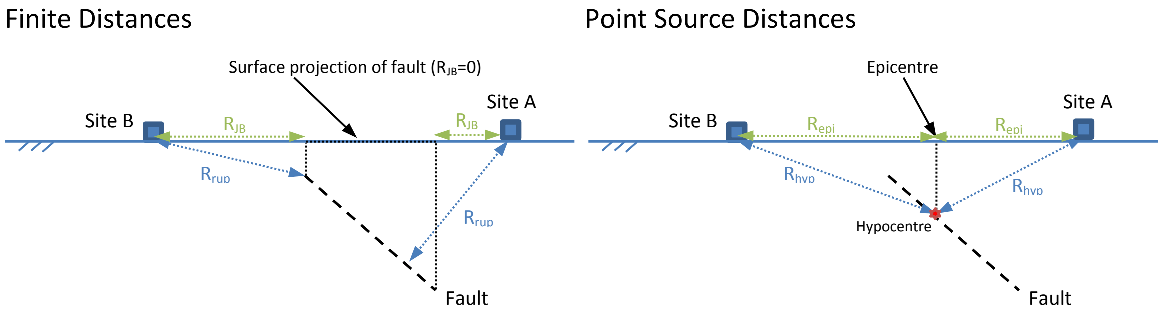

Figure 9: Distance metrics. Cross section of a scenario for a buried fault. Left: finite measures of distance; right: point source measures of distance.

There are two main groups of commonly used distance metrics: point source and finite fault measures as summarized in Figure 9. Point source distance metrics include:

- hypocentral distance (R_{hyp}): the slant distance between source hypocentre and site;
- epicentral distance (R_{epi}): the horizontal distance between the surface projection of the hypocentre and the site.

Finite fault distances commonly used are:

- rupture distance (R_{rup}): shortest distance from the rupture to the site;
- Joyner-Boore distance (R_{JB}): shortest distance from the surface projection of the rupture to the site.

Point source distance measures result in concentric circles defining contours of equal ground-motion at the surface for a scenario event. Finite source distance measures result in elongated contours around a line source. For this reason, point source measures tend not to be used as often as finite measures, since the latter result in a more realistic spatial ground-motion distribution for larger magnitude events. However, it may be argued that point-source measures are more robust (since no knowledge of the rupture plane is required): introducing finite measures may not necessarily reduce the misfit of the prediction model to the dataset. Furthermore, depending on the user's implementation may call for the use of point source distances – in this case finite fault distance models present a disadvantage, since the input first has to be converted to a point-source measure including propagated uncertainty. As a result some authors have started providing multiple options for distance metrics (e.g., Akkar *et al.*, 2014a).

Finite fault measures are by far the most common distance metric used for GMPEs. The Joyner-Boore distance, similarly to epicentral distance, is independent of the source depth: for instance, the same distance of zero is obtained directly above two earthquakes at depths of 1km and 30km. The resulting predictions from models using R_{JB} are therefore coupled to the depth distribution of events used in a GMPE's derivation. For locally derived models this may not be an issue, however using a model developed with tectonic activity to predict ground motion from shallow induced seismicity will introduce bias. Considering near-fault ground-motions may be strongly influenced by source depth this can be seen as a disadvantage. On the other hand, it must also be considered that source depth is rarely known to a high degree of accuracy.

The rupture distance implicitly accounts for source depth (deeper faults are further away and hence lead to lower ground-motions) and is therefore more physically realistic. Models developed using this metric decouple the source depth distribution in the database used to derive them. As a result they may be more applicable to different regions. Despite its advantages rupture distance is more uncertain to obtain for real recordings. Furthermore, effects such as increased ground-motion on the hanging wall must be explicitly accounted for when using rupture distance (Figure 3).

5 Regression and Uncertainties

GMPEs are multi-degree of freedom models that require careful fitting in order to derive robust coefficients and avoid trade-offs between the source, path and site components. Typically the fitting of the GMPE to the data is done using a multi-stage maximum likelihood approach (Joyner and Boore, 1993) or more commonly for recent GMPEs, the random-effects approach (Abrahamson and Youngs, 1992). The misfit of a GMPE to the data used to derive it (represented as the standard-deviation of log-space residuals, σ_T) is considered as total uncertainty. σ_T is then split into at least between-event (also called inter-event) uncertainty, τ, and within-event (or intra-event) uncertainty, φ, in order to isolate event-specific and path-site specific aleatory variability (randomness):

$$\sigma_T = \sqrt{\tau^2 + \varphi^2}) \tag{4}$$

This is an important feature used in seismic hazard analysis to appropriately incorporate the lower variability ground-motion expected from a single event (φ), with respect to the average variability over many events (σ_T) (Figure 10).

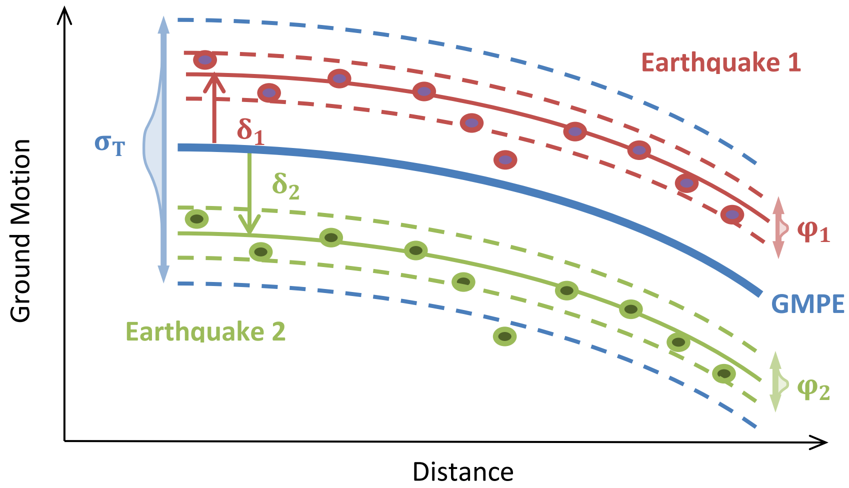

Figure 10: Schematic representation of GMPE uncertainties. Blue: GMPE (solid = median; dashed = $\pm\sigma_T$ [total uncertainty]). Red: earthquake 1 with $\delta_1 \pm \varphi_1$ offset from GMPE median. Green: earthquake 2 with $\delta_2 \pm \varphi_2$ offset from GMPE median. The standard deviation of $\delta_{1...N}$ gives τ in equation (4). The average of $\varphi_{1...N}$ gives φ in equation (4).

Recent work has shown the importance of further decoupling uncertainly in GMPEs and the subsequent removal of the ergodic assumption (Rodriguez-Marek *et al.*, 2013). The ergodic assumption used to develop GMPEs is that the ground-motion observed in the spatial domain (i.e., over numerous recording sites) is reflective of the ground-motion observed in the time-domain (i.e., at one site). A problem with this approach is that site-to-site variability is mapped into the within-event uncertainty measure of GMPEs. However, when computing hazard, or simply examining scenario events, we use a reference site (either known or theoretical). Including site-to-site variability in predictions therefore unjustifiably increases the overall prediction uncertainty for many applications.

The reality is that in many cases we know the expected site response behaviour and its uncertainty. In this case the so-called single site sigma (σ_{SS}) can significantly reduce the predicted ground-motion variability and the resultant long-return period hazard (Atkinson, 2006). Single site sigma is given by:

$$\sigma_{SS} = \sqrt{\tau^2 + \varphi_{SS}{}^2)} \tag{5}$$

where φ_{SS} is the within-event uncertainty for a single site: the standard deviation of ground-motions observed if we were to record a single earthquake on multiple clones of a given site (at various azimuths, distances, etc.) (Figure 11). Rodriguez-Marek et al. (2013) determined φ_{SS} for a variety of regions (including Switzerland) and found it appears to be mostly independent of location. They proposed four models to describe φ_{SS}: period dependent, distance-period dependent, magnitude-period dependent and magnitude-distance-period dependent. Physical reasons for magnitude and distance dependence of ground-motion variability do support a higher variability of ground-motion in the near-field ($R \lesssim 30\ km$), where complex and highly variable source effects are often observed (e.g., directivity), and for smaller earthquakes which tend to exhibit more variability than larger events (e.g., in terms of source depth, stress-drop, etc.).

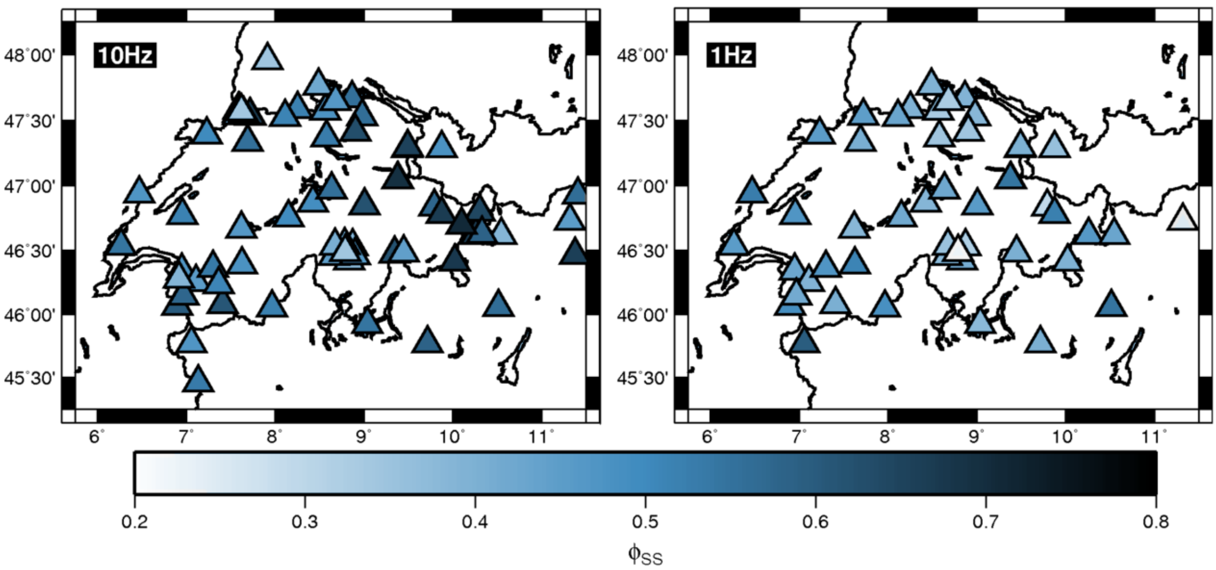

Figure 11: φ_{SS} (natural log units) for different sites in Switzerland at 1 and 10Hz (Edwards and Fäh, 2013b).

The uncertainty between models such as median ground-motion or φ_{SS} is a common feature of seismic hazard. For instance, due to a lack of data (particularly high magnitude, short distance), Rodriguez-Marek et al. (2013) did not recommend a best φ_{SS} model. For hazard these different models therefore manifest as a source of epistemic uncertainty which has to be accommodated, for example, through logic tree approaches. Nevertheless, with increasing data recorded in coming years, and further scientific analysis, this uncertainty can be reduced, with logic-tree branches being down-weighted or ultimately removed.

6 GMPEs in Switzerland

Switzerland presents a common case of moderate seismic hazard due to large events (M ~ 6) on the time-scale of the order 100 years. On average, about 10 earthquakes are felt each year, with damaging events expected every 5–10 years (Wiemer *et al.*, 2009). However, due to a limited period of monitoring (since around the start of the 21st century for the fully digital seismic networks), few large regional events have yet been recorded. The largest recorded events have all occurred outside Swiss borders: the St. Dié, France, earthquake with M_L 5.8 (M_w 4.8); the Bormio, Italy, event with M_L 4.9 (M_w 4.9); and the Salò, Italy, event with M_L 5.0 (M_w 5.0). Choosing suitable GMPEs for Switzerland is difficult due to this lack of recorded strong-motion data. There are two broad approaches that have been adopted: the adjustment of empirically derived GMPEs (based on data from more seismically active regions), or the simulation of ground-motion recordings with a model that is calibrated with small earthquakes.

Several GMPEs have been used in recent years in Switzerland (Table 1). The SHARE project split Switzerland into two broad tectonic regions, stable continental to the north, and shallow active to the south. Such a distinction is strongly debatable, however GMPEs used for the two regions had a great deal of overlap (Table 1). The Probabilistic Seismic Hazard Analysis for Swiss Nuclear Power Plant Sites (PEGASOS) Refinement Project was only concerned with hazard at nuclear power stations in the Swiss Foreland, while the Swiss Hazard 2014 project uses the same empirical models across Switzerland, whilst using different simulation based models from Edwards and Fäh (2013b) to distinguish between ground motion related to Swiss Foreland and Alpine seismicity.

The selection of GMPEs for seismic hazard generally focuses on covering the epistemic uncertainty: the fact that we assume no single model can perfectly predict median ground-motion. Several recent GMPEs have been developed using the Next Generation Attenuation (NGA) database (Power *et al.*, 2008), based on global earthquakes, with a focus on Californian events at smaller magnitudes. The NGA database has recently been updated to the NGA West 2 (Bozorgnia *et al.*, 2014, Ancheta *et al.*, 2014) dataset and related models (currently in press at the time of this report). A recent European based strong motion database RESORCE (Akkar *et al.*, 2014b) has also led to the publication of several European specific GMPEs (Douglas *et al.*, 2014 and references therein). In seismic hazard projects a subset of relations from a given strong-motion dataset (e.g., NGA) is usually chosen, since the background datasets usually overlap significantly and lead to similar models.

Table 1: Overview of GMPEs used in recent seismic hazard projects in Switzerland. * indicates simulation based models.
• GMPEs that were used, (•) GMPEs that were evaluated but not used.

	SHARE (stable continental)	SHARE (shallow active)	PRP	Swiss Hazard 2014	Reference
AB06 *			(•)		(Atkinson and Boore, 2006)
AB10	•	•	•	•	(Akkar and Bommer, 2010)
AC10			•		(Akkar and Cagnan, 2010)
AS08			•		(Abrahamson and Silva, 2008)
BA08			•		(Boore and Atkinson, 2008)
BETAL11			(•)		(Bindi *et al.*, 2011)
CA03 *	•				(Campbell, 2003)
CB08			•		(Campbell and Bozorgnia, 2008)
CF08	•	•		•	(Cauzzi and Faccioli, 2008)
CY08	•	•	•	•	(Chiou and Youngs, 2008)
TO02 *	•		(•)		(Toro *et al.*, 1997)
ZETAL06		•	•	•	(Zhao *et al.*, 2006)
EF13 *			•	•	(Edwards and Fäh, 2013b)

7 GMPE Adjustment

7.1 V_s-κ (shear-wave velocity and site specific attenuation)

GMPEs provide median ground motion at a given site condition. This is typically based on site class or Vs30 for empirical models (CEN, 2004, BSSC, 2003), or velocity/material property profiles in the case of simulation models (e.g., Poggi *et al.*, 2011, Poggi *et al.*, 2013, Boore and Joyner, 1997). It is commonly accepted that site conditions have a dominant effect on the seismic wave-field. Even within a single site class (or Vs30 range), significant variation in amplification is apparent (e.g., Edwards *et al.*, 2013). For site or reference specific analyses, therefore, careful attention should be paid to accounting for the effect of the local subsurface. In site specific hazard projects such as PEGASOS Refinement, GMPEs were required to predict at a predefined bedrock condition, such that results from site response analyses could be applied subsequently. In the Swiss Hazard 2014 project, maps are produced at a reference rock velocity profile (Poggi *et al.*, 2011), while in SHARE results were broadly referenced to a Vs30=800m/s site class (Delavaud *et al.*, 2012).

Empirical GMPEs are not reliable at high Vs30 since they are based on incomplete (or limited) datasets, dominated by low Vs30 sites. Additionally they do not explicitly account for the effects of attenuation in the near surface. Nevertheless empirical GMPEs can be used at moderate Vs30 values (based on assessment of input data) and adjustment performed to correct predictions to the bedrock level (e.g., PEGASOS Refinement, Swiss Hazard 2014). This has typically been accomplished in the past using the hybrid empirical approach (Campbell, 2003): the ratio between stochastic simulation models using host and target specific inputs are used to adjust the empirical GMPE. However, this approach has been shown to be unstable when large differences in near-surface attenuation are expected. An alternative approach to adjust GMPEs was developed by Al Atik et al. (2014). This approach uses inverse random vibration theory (Rathje *et al.*, 2005) to estimate equivalent Fourier spectrum models from GMPEs, which can then be adjusted with simple ratios between anelastic site response in the host and target regions. Figure 12 shows examples of the possible V_s-κ corrections to a Swiss reference model for the Akkar and Bommer (2010) GMPE. Note that the correction is strongest at short periods (T < 0.1s) and is most sensitive to the change in site attenuation (κ). The suite of possible corrections represents the significant epistemic uncertainty involved.

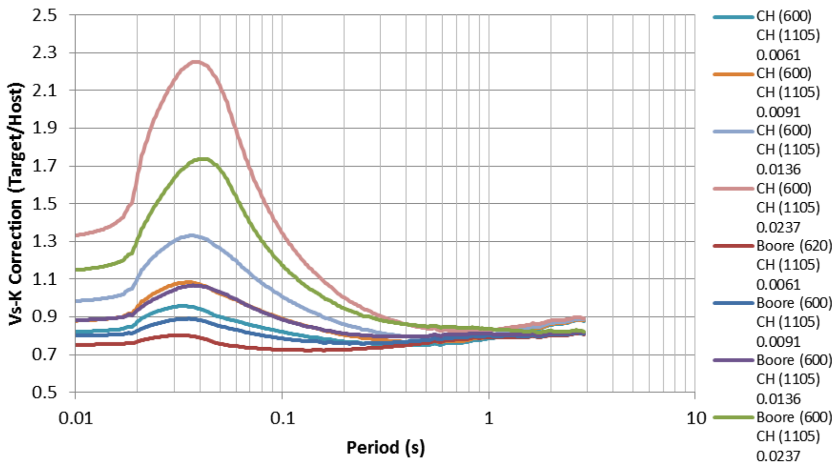

Figure 12: Example of a range of possible V_s-κ corrections to a Swiss reference for the model of Akkar and Bommer (2010). The legend indicates, from top to bottom for each line, the host model (and Vs30), the target model (and Vs30) and the decrease in κ (in s). CH refers to the model of Poggi et al. (2011) and Boore refers to the model of Boore and Joyner (1997).

7.2 Small magnitude adjustments

Empirical GMPEs are derived from dataset with relatively large magnitude earthquakes ($\boldsymbol{M} \gtrsim 4.5$), since the metadata (magnitude, depth, distance to fault, etc.) for such events are typically well known. For smaller events this information is more uncertain. Authors that have included small magnitude data in GMPE development (e.g., Chiou *et al.*, 2010, Bommer *et al.*, 2007) have concluded that: (1) GMPEs should be derived using data at least one magnitude unit below that required for their target application and (2) the aleatory variability significantly increases as a result of including small magnitude data.

Since some hazard projects use minimum hazard integration magnitude lower than that used for GMPE development they should be adjusted if they are not already suitable for prediction at these magnitudes. An approach recently adopted for this purpose is the so called 'small magnitude adjustment' (SMA). We assume that the GMPE is valid between some magnitude range (depending on the data used to derive the model, e.g., $5.5 < \boldsymbol{M} < 7.5$) and then adjust the magnitude scaling such that it is consistent with locally recorded data when using appropriate magnitudes. An example of the small magnitude adjustment as applied, for instance in PRP, (Stafford, 2011) is:

$$\delta(M,R|T) = \left(\frac{M_{ref} - M}{a}\right)^b \left(c + d\,ln\left(\frac{R}{R_{ref}}\right)\right), \quad M \leq M_{ref} \qquad (6)$$

$$\delta(M,R|T) = 0, \quad M > M_{ref}$$

Where the adjusted GMPE is given as:

$$Y_{SMA} = Y - \delta(M,R|T) \qquad (7)$$

With Y the original GMPE prediction (log-space output). M_{ref} is chosen based on the magnitude above which the GMPE is trusted. R_{ref} is a generic distance chosen as a reference while the coefficients (a…d) are determined by examining the residual misfit of a specific GMPE to the locally recorded small magnitude data.

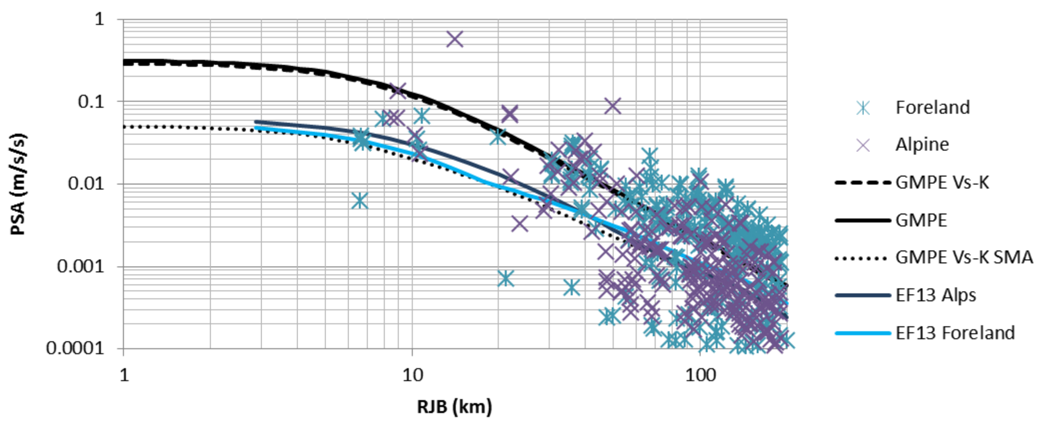

Figure 13: Example of small magnitude adjustment applied to the model of Akkar and Bommer (2010). Recorded Swiss foreland and alpine data for events with 3.3≤M≤3.7 are shown (symbols). The original GMPE (for M3.5) is shown as the solid black line and over-predicts the median of the data. The corrected GMPE (GMPE Vs-k SMA) is shown to match the data distribution and the model Swiss model of Edwards and Fäh (EF13; 2013). The SMA is much stronger than the Vs-k adjustment for small magnitude events.

Outlook and Future Trends

The prediction of ground-motion still presents a high degree of uncertainty due to a combination of natural randomness (aleatory variability) and limitations in modelling or scientific understanding (epistemic uncertainty). In recent years, significant progress has been made by reducing the predicted aleatory component of ground-motion and, instead, assigning epistemic uncertainty through logic tree approaches (e.g., using several GMPEs, adjustment strategies, etc.). While the uncertainty has shifted to a potentially reducible component, the overall uncertainty in hazard has not been significantly reduced (Strasser *et al.*, 2009). Future work in ground-motion prediction should focus on reducing the epistemic uncertainty included in PSHA. Several areas of current research present a promising outlook for the further reduction of epistemic uncertainty through better understanding of physical processes, in addition to improved modelling and simulation approaches. These topics include:

1. The collection and archival of improved (more reliable) metadata, such as site velocity and material property profiles and fault information for smaller events. Detailed site characterisation will allow us to properly account for site amplification (including 1D, 2D and 3D response) and non-linear behaviour. This will reduce the ground-motion uncertainty determined during GMPE derivation and improve the reliability of forward modelling approaches. More reliable fault information (including for smaller events) will allow more events to be included in GMPE development, extending the range of magnitudes available to determine appropriate scaling to both lower and higher magnitudes resulting in more robust GMPEs.
2. The focus on development of GMPEs for predicting Fourier spectral estimates and duration (rather than directly response spectral ordinates, e.g., PSA), so that local corrections (e.g., for site amplification and attenuation) are simplified (Bora *et al.*, 2013). Response spectra are computed in a final step for engineering applications. This will significantly reduce the epistemic uncertainty of adjusting response spectra, a key issue highlighted during the PEGASOS Refinement project.
3. A shortage of data in the near-field of earthquakes and for large events still limits the applicability of empirical GMPEs. The trend for ground-motion prediction moves towards reliable hybrid simulation based approaches (Mai *et al.*, 2010, Graves and Pitarka, 2010), calibrated on existing data, so that such data shortages (e.g., near-field, high magnitude) can be avoided. However, this field still has a significant way to go before being included in probabilistic seismic hazard analyses: currently the understanding of appropriate input parameters and their covariance leads to results that are inconsistent with empirical observations (e.g., high variability, decrease of ground-motion near faults).
4. The understanding of interaction of topographic site effects on ground-motion. For instance, a recent study (Burjanek *et al.*, 2014) showed that observed ground motion amplification at sites with pronounced topography is tightly linked with the local sub-surface structure rather than the geometrical effect of the surface alone. Standalone analysis of the terrain geometry in the absence of reliable shear wave velocity models (point 1) will therefore lead to severe underestimation of potential amplification.

References

Abrahamson, N. and W. Silva (2008). Summary of the abrahamson & silva nga ground-motion relations, *Earthq Spectra* **24**, 67-97

Abrahamson, N. A. and P. G. Somerville (1996). Effects of the hanging wall and footwall on ground motions recorded during the northridge earthquake, *B Seismol Soc Am* **86**, S93-S99

Abrahamson, N. A. and R. R. Youngs (1992). A stable algorithm for regression-analyses using the random effects model, *B Seismol Soc Am* **82**, 505-510

Akkar, S. and J. J. Bommer (2010). Empirical equations for the prediction of pga, pgv, and spectral accelerations in europe, the mediterranean region, and the middle east, *Seismol Res Lett* **81**, 195-206

Akkar, S. and Z. Cagnan (2010). A local ground-motion predictive model for turkey, and its comparison with other regional and global ground-motion models, *B Seismol Soc Am* **100**, 2978-2995

Akkar, S., M. A. Sandikkaya and J. J. Bommer (2014a). Empirical ground-motion models for point- and extended-source crustal earthquake scenarios in europe and the middle east, *B Earthq Eng* **12**, 359-387

Akkar, S., M. A. Sandikkaya, M. Senyurt, A. A. Sisi, B. O. Ay, P. Traversa, J. Douglas, F. Cotton, L. Luzi, B. Hernandez and S. Godey (2014b). Reference database for seismic ground-motion in europe (resorce), *B Earthq Eng* **12**, 311-339

Al Atik, L., A. Kottke, N. Abrahamson and J. Hollenback (2014). Kappa (kappa) scaling of ground-motion prediction equations using an inverse random vibration theory approach, *B Seismol Soc Am* **104**, 336-346

Ancheta, T. D., R. B. Darragh, J. P. Stewart, E. Seyhan, W. J. Silva, B. S. Chiou, K. E. Wooddell, R. W. Graves, A. R. Kottke and D. M. Boore (2014). Nga-west 2 database, *Earthq Spectra*

Atkinson, G. M. (1993). Earthquake source spectra in eastern north-america, *B Seismol Soc Am* **83**, 1778-1798

Atkinson, G. M. (2006). Single-station sigma, *B Seismol Soc Am* **96**, 446-455

Atkinson, G. M. and D. M. Boore (2006). Earthquake ground-motion prediction equations for eastern north america, *B Seismol Soc Am* **96**, 2181-2205

Bindi, D., F. Pacor, L. Luzi, R. Puglia, M. Massa, G. Ameri and R. Paolucci (2011). Ground motion prediction equations derived from the italian strong motion database, *B Earthq Eng* **9**, 1899-1920

Bommer, J. J., S. Akkar and O. Kale (2011). A model for vertical-to-horizontal response spectral ratios for europe and the middle east, *B Seismol Soc Am* **101**, 1783-1806

Bommer, J. J., J. Douglas, F. Scherbaum, F. Cotton, H. Bungum and D. Fah (2010). On the selection of ground-motion prediction equations for seismic hazard analysis, *Seismol Res Lett* **81**, 783-793

Bommer, J. J., P. J. Stafford, J. E. Alarcon and S. Akkar (2007). The influence of magnitude range on empirical ground-motion prediction, *B Seismol Soc Am* **97**, 2152-2170

Boore, D. M. (2003). Simulation of ground motion using the stochastic method, *Pure Appl Geophys* **160**, 635-676

Boore, D. M. (2009). Comparing stochastic point-source and finite-source ground-motion simulations: Smsim and exsim, *B Seismol Soc Am* **99**, 3202-3216

Boore, D. M. and G. M. Atkinson (2008). Ground-motion prediction equations for the average horizontal component of pga, pgv, and 5%-damped psa at spectral periods between 0.01 s and 10.0 s, *Earthq Spectra* **24**, 99-138

Boore, D. M. and W. B. Joyner (1997). Site amplifications for generic rock sites, *B Seismol Soc Am* **87**, 327-341

Bora, S., F. Scherbaum, N. Kuehn and P. Stafford (2013). Fourier spectral- and duration models for the generation of response spectra adjustable to different source-, propagation-, and site conditions, *B Earthq Eng*, 1-27

Bozorgnia, Y., N. A. Abrahamson, L. A. Atik, T. D. Ancheta, G. M. Atkinson, J. W. Baker, A. Baltay, D. M. Boore, K. W. Campbell and B. S.-J. Chiou (2014). Nga-west2 research project, *Earthq Spectra*

Brune, J. N. (1970). Tectonic stress and spectra of seismic shear waves from earthquakes, *J Geophys Res* **75**, 4997-5009

Brune, J. N. (1971). Correction, *J Geophys Res* **76**, 5002

BSSC (2003). The 2003 nehrp recommended provisions for new buildings and other structures, part 1: Provisions (fema 450), Building Seismic Safety Council, Washington.

Burjanek, J., B. Edwards and D. Fah (2014). Empirical evidence of local seismic effects at sites with pronounced topography: A systematic approach, *Geophys J Int* **197**, 608-619

Campbell, K. W. (2003). Prediction of strong ground motion using the hybrid empirical method and its use in the development of ground-motion (attenuation) relations in eastern north america, *B Seismol Soc Am* **93**, 1012-1033

Campbell, K. W. and Y. Bozorgnia (2003). Updated near-source ground-motion (attenuation) relations for the horizontal and vertical components of peak ground acceleration and acceleration response spectra (vol 93, pg 314, 2003), *B Seismol Soc Am* **93**, 1872-1872

Campbell, K. W. and Y. Bozorgnia (2008). Nga ground motion model for the geometric mean horizontal component of pga, pgv, pgd and 5% damped linear elastic response spectra for periods ranging from 0.01 to 10 s, *Earthq Spectra* **24**, 139-171

Cartwright, D. E. and M. S. Longuet-Higgins (1956). The statistical distribution of the maxima of a random function, *Proc R Soc Lon Ser-A* **237**, 212-232

Cauzzi, C., B. Edwards, D. Fäh, J. Clinton, S. Wiemer, P. Kästli, G. Cua and D. Giardini (submitted, 2014). New predictive equations and site amplification estimates for the next-generation swiss shakemaps., *submitted to Geophysical Journal International*

Cauzzi, C. and E. Faccioli (2008). Broadband (0.05 to 20 s) prediction of displacement response spectra based on worldwide digital records, *J Seismol* **12**, 453-475

CEN (2004). Eurocode 8: Design of structures for earthquake resistance—part 1: General rules, seismic actions and rules for buildings. *in Eurocode 8*, European Committee for Standardization, Brussels.

Chiou, B., R. Youngs, N. Abrahamson and K. Addo (2010). Ground-motion attenuation model for small-to-moderate shallow crustal earthquakes in california and its implications on regionalization of ground-motion prediction models, *Earthq Spectra* **26**, 907-926

Chiou, B. S. J. and R. R. Youngs (2008). An nga model for the average horizontal component of peak ground motion and response spectra, *Earthq Spectra* **24**, 173-215

Cotton, F., G. Pousse, F. Bonilla and F. Scherbaum (2008). On the discrepancy of recent european ground-motion observations and predictions from empirical models: Analysis of kik-net accelerometric data and point-sources stochastic simulations, *B Seismol Soc Am* **98**, 2244-2261

Cotton, F., F. Scherbaum, J. J. Bommer and H. Bungum (2006). Criteria for selecting and adjusting ground-motion models for specific target regions: Application to central europe and rock sites, *J Seismol* **10**, 137-156

Delavaud, E., F. Cotton, S. Akkar, F. Scherbaum, L. Danciu, C. Beauval, S. Drouet, J. Douglas, R. Basili, M. A. Sandikkaya, M. Segou, E. Faccioli and N. Theodoulidis (2012). Toward a ground-motion logic tree for probabilistic seismic hazard assessment in europe, *J Seismol* **16**, 451-473

Douglas, J. (2011). Ground-motion prediction equations 1964-2010Pacific Earthquake Engineering Research Center (PEER),

Douglas, J. (2014). Ground motion prediction equations 1964-2014. *in Second European Conference on Eathquake Engineering and Seismology*, Istanbul, Turkey, 24-29 August, 2014.

Douglas, J., S. Akkar, G. Ameri, P.-Y. Bard, D. Bindi, J. J. Bommer, S. S. Bora, F. Cotton, B. Derras and M. Hermkes (2014). Comparisons among the five ground-motion models developed using resorce for the prediction of response spectral accelerations due to earthquakes in europe and the middle east, *B Earthq Eng* **12**, 341-358

Edwards, B. and D. Fäh (2013a). Measurements of stress parameter and site attenuation from recordings of moderate to large earthquakes in europe and the middle east, *Geophys J Int* **194**, 1190-1202

Edwards, B. and D. Fäh (2013b). A stochastic ground-motion model for switzerland, *B Seismol Soc Am* **103**, 78-98

Edwards, B., D. Fäh and D. Giardini (2011a). Attenuation of seismic shear wave energy in switzerland, *Geophys J Int* **185**, 967-984

Edwards, B., C. Michel, V. Poggi and D. Fäh (2013). Determination of site amplification from regional seismicity: Application to the swiss national seismic networks, *Seismol Res Lett* **84**, 611-621

Edwards, B., V. Poggi and D. Fäh (2011b). A predictive equation for the vertical-to-horizontal ratio of ground motion at rock sites based on shear-wave velocity profiles from japan and switzerland, *B Seismol Soc Am* **101**, 2998-3019

Fäh, D., S. Fritsche, V. Poggi, G. Gassner-Stamm, P. Kästli, J. Burjanek, P. Zweifel, S. Barman, J. Clinton, L. Keller, P. Renault and S. Heuberger (2009). Determination of site information for seismic stations in switzerland, Swiss Seismological Service Technical Report: SED/PRP/R/004/20090831 for the swissnuclear PEGASOS Refinement Project,

Fukushima, Y. (1996). Scaling relations for strong ground motion prediction models with m(2) terms, *B Seismol Soc Am* **86**, 329-336

Graves, R. W. and A. Pitarka (2010). Broadband ground-motion simulation using a hybrid approach, *B Seismol Soc Am* **100**, 2095-2123

Gulerce, Z. and N. A. Abrahamson (2011). Site-specific design spectra for vertical ground motion, *Earthq Spectra* **27**, 1023-1047

Joyner, W. B. and D. M. Boore (1993). Methods for regression-analysis of strong-motion data, *B Seismol Soc Am* **83**, 469-487

Knopoff, L. (1964). Q, *Rev Geophys* **2**, 625-660

Madariaga, R. (1976). Dynamics of an expanding circular fault, *B Seismol Soc Am* **66**, 639-666

Mai, P. M., W. Imperatori and K. B. Olsen (2010). Hybrid broadband ground-motion simulations: Combining long-period deterministic synthetics with high-frequency multiple s-to-s backscattering, *B Seismol Soc Am* **100**, 2124-2142

Michel, C., B. Edwards, V. Poggi, J. Burjanek, D. Roten, C. Cauzzi and D. Fäh (2014). Assessment of site effects in alpine regions through systematic site characterization of seismic stations, *B Seismol Soc Am*, (accepted)

Morozov, I. B. (2008). Geometrical attenuation, frequency dependence of q, and the absorption band problem, *Geophys J Int* **175**, 239-252

Motazedian, D. and G. M. Atkinson (2005). Stochastic finite-fault modeling based on a dynamic corner frequency, *B Seismol Soc Am* **95**, 995-1010

Poggi, V., B. Edwards and D. Fäh (2011). Derivation of a reference shear-wave velocity model from empirical site amplification, *B Seismol Soc Am* **101**, 258-274

Poggi, V., B. Edwards and D. Fäh (2012a). Characterizing the vertical-to-horizontal ratio of ground motion at soft-sediment sites, *B Seismol Soc Am* **102**, 2741-2756

Poggi, V., B. Edwards and D. Fäh (2013). Reference s-wave velocity profile and attenuation models for ground-motion prediction equations: Application to japan, *B Seismol Soc Am* **103**, 2645-2656

Poggi, V., D. Fäh, J. Burjanek and D. Giardini (2012b). The use of rayleigh-wave ellipticity for site-specific hazard assessment and microzonation: Application to the city of lucerne, switzerland, *Geophys J Int* **188**, 1154-1172

Power, M., B. Chiou, N. Abrahamson, Y. Bozorgnia, T. Shantz and C. Roblee (2008). An overview of the nga project, *Earthq Spectra* **24**, 3-21

Rathje, E., A. Kottke and C. Ozbey (2005). Using inverse random vibration theory to develop input fourier amplitude spectra for use in site response, *16th International Conference on Soil Mechanics and Geotechnical Eningeering: TC4 Earthquake Geotechnical Engineering Satellite Conference*, 160-166

Rietbrock, A., F. Strasser and B. Edwards (2013). A stochastic earthquake ground-motion prediction model for the united kingdom, *B Seismol Soc Am* **103**, 57-77

Rodriguez-Marek, A., F. Cotton, N. A. Abrahamson, S. Akkar, L. Al Atik, B. Edwards, G. A. Montalva and H. M. Dawood (2013). A model for single-station standard deviation using data from various tectonic regions, *B Seismol Soc Am* **103**, 3149-3163

Scherbaum, F., J. Schmedes and F. Cotton (2004). On the conversion of source-to-site distance measures for extended earthquake source models, *B Seismol Soc Am* **94**, 1053-1069

Stafford, P. (2011). Procedure for small-magnitude extension of gmpes, pp. 25, Imperial College London,

Strasser, F. O., N. A. Abrahamson and J. J. Bommer (2009). Sigma: Issues, insights, and challenges, *Seismol Res Lett* **80**, 40-56

Toro, G. R., N. A. Abrahamson and J. F. Schneider (1997). Model of strong ground motions from earthquakes in central and eastern north america: Best estimates and uncertainties, *Seismol Res Lett* **68**, 41-57

Wiemer, S., D. Giardini, D. Fah, N. Deichmann and S. Sellami (2009). Probabilistic seismic hazard assessment of switzerland: Best estimates and uncertainties, *J Seismol* **13**, 449-478

Zhao, J. X. and M. Lu (2011). Magnitude-scaling rate in ground-motion prediction equations for response spectra from large, shallow crustal earthquakes, *B Seismol Soc Am* **101**, 2643-2661

Zhao, J. X., J. Zhang, A. Asano, Y. Ohno, T. Oouchi, T. Takahashi, H. Ogawa, K. Irikura, H. K. Thio, P. G. Somerville, Y. Fukushima and Y. Fukushima (2006). Attenuation relations of strong ground motion in japan using site classification based on predominant period, *B Seismol Soc Am* **96**, 898-913

Appendix A

Relevant Technical Reports and Journal Articles by the Swiss Seismological Service

A significant number of *technical reports* and ***journal articles*** were produced by the Swiss Seismological Service over the period 2009-2014 as part of the Pegasos Refinement Project and the ENSI Strong Ground-Motion Expert Group. These articles are available upon request and are listed by topic (with limited repetition) here.

Strong Ground Motion in Switzerland

Edwards, B. and D. Fäh (2013). A stochastic ground-motion model for switzerland, *B Seismol Soc Am* **103**, 78-98.

Edwards, B., D. Fäh, J. Burjánek and G. Cua (2009). New Earthquake Data: Strong Motion Recorded at swissnuclear Power Plants. Technical Report SED/PRP/R/001/20090608.

Edwards, B., D. Fäh, N. Deichmann (2009). Response Spectra of New Acceleration Waveforms. Technical Report SED/PRP/R/002/20090622.

Edwards, B., D. Fäh, B. Allmann, V. Poggi (2010). Stochastic ground motion model for Switzerland. Technical Report SED/PRP/R/006/20100526.

Earthquake Source

Edwards, B., B. Allmann, D. Fäh and J. Clinton (2010). Automatic computation of moment magnitudes for small earthquakes and the scaling of local to moment magnitude, *Geophys J Int* **183**, 407-420.

Goertz-Allmann, B. P., B. Edwards, F. Bethmann, N. Deichmann, J. Clinton, D. Fäh and D. Giardini (2011). A new empirical magnitude scaling relation for switzerland, *B Seismol Soc Am* **101**, 3088-3095.

Edwards, B. and D. Fäh (2013). Measurements of stress parameter and site attenuation from recordings of moderate to large earthquakes in europe and the middle east, *Geophys J Int* **194**, 1190-1202.

Goertz-Allmann, B. P. and B. Edwards (2014). Constraints on crustal attenuation and three-dimensional spatial distribution of stress drop in switzerland, *Geophys J Int* **196**, 493-509.

Allmann, B., B. Edwards, and N. Deichmann (2009). Work Package 2: Source studies. Technical Report SED/PRP/R/003/20090828.

Edwards, B., D. Fäh (2010). Extrapolation of Swiss Stochastic Ground Motion Model. Technical Report SED/PRP/R/020/20101107.

Allmann, B., B. Edwards, F. Bethmann and N. Deichmann (2010). ECOS09 Appendix I Determination of MW and calibration of ML (SED)–MW regression. Swiss Seismological Service ETH Zurich Report SED/ECOS/R/001/20110417.

Site

Poggi, V., B. Edwards and D. Fäh (2011). Derivation of a reference shear-wave velocity model from empirical site amplification, *B Seismol Soc Am* **101**, 258-274.

Edwards, B. and D. Fäh (2013). Measurements of stress parameter and site attenuation from recordings of moderate to large earthquakes in europe and the middle east, *Geophys J Int* **194**, 1190-1202.

Edwards, B., C. Michel, V. Poggi and D. Fäh (2013). Determination of site amplification from regional seismicity: Application to the swiss national seismic networks, *Seismol Res Lett* **84**, 611-621.

Poggi, V., B. Edwards and D. Fäh (2013). Reference s-wave velocity profile and attenuation models for ground-motion prediction equations: Application to japan, *B Seismol Soc Am* **103**, 2645-2656.

Poggi, V., J. Burjánek, B. Edwards and D. Fäh (2013). SED Extended Velocity Profiles at Rock Sites. Technical Report SED/PRP/R/039/20130822.

Poggi, V., B. Edwards and D. Fäh (2012). Empirical estimation of kappa from rock velocity profiles at the Swiss NPP sites. Technical Report SED/PRP/R/036/20121217.

Edwards, B. and D. Fäh (2012). Site Specific Kappa. Technical Report SED/PRP/R/035/20120320.

Edwards, B. and D. Fäh (2011). Note on the Relation of ϕ_{ss} to Station Back-Azimuth Coverage in Swiss Data. Technical Report SED/PRP/R/034/20111222.

Poggi, V. and D. Fäh (2013), Calibration of a reference profile for host-to-target correction of ground motion models, Technical Report SED/PRP/R/40/20131007

Path

Edwards, B., D. Fäh and D. Giardini (2011). Attenuation of seismic shear wave energy in switzerland, *Geophys J Int* **185**, 967-984.

Goertz-Allmann, B. P. and B. Edwards (2014). Constraints on crustal attenuation and three-dimensional spatial distribution of stress drop in switzerland, *Geophys J Int* **196**, 493-509.

Edwards, B. and D. Fäh (2011). Sensitivity of R_{EFF} Simulations. Technical Report SED/PRP/R/032/20111108.

Edwards, B. and D. Fäh (2010). Computation of Q and κ for use in the correction of GMPE to a Swiss reference. Technical Report SED/PRP/R/007/20101801.

Vertical to Horizontal Ground Motion Ratio

Edwards, B., V. Poggi and D. Fäh (2011). A predictive equation for the vertical-to-horizontal ratio of ground motion at rock sites based on shear-wave velocity profiles from japan and switzerland, *B Seismol Soc Am* **101**, 2998-3019.

Poggi, V., B. Edwards and D. Fäh (2012). Characterizing the vertical-to-horizontal ratio of ground motion at soft-sediment sites, *B Seismol Soc Am* **102**, 2741-2756.

Edwards, B. and D. Fäh (2011). Note on the Relation of κ to V/H in Swiss/Japanese Data. Technical Report SED/PRP/R/033/20111223.

Uncertainty

Rodriguez-Marek, A., F. Cotton, N. A. Abrahamson, S. Akkar, L. Al Atik, B. Edwards, G. A. Montalva and H. M. Dawood (2013). A model for single-station standard deviation using data from various tectonic regions, *B Seismol Soc Am* **103**, 3149-3163.